Multivariable Model Predictive Control of Thin Film Surface Roughness and Slope for Light Trapping Optimization

Xinyu Zhang,[†] Gangshi Hu,[†] Gerassimos Orkoulas,[†] and Panagiotis D. Christofides*[,†,‡]

Department of Chemical and Biomolecular Engineering and Department of Electrical Engineering, University of California, Los Angeles, California 90095

This work focuses on the development of a multivariable model predictive controller that simultaneously regulates thin film surface roughness and mean slope to optimize light reflectance and transmittance during thin film manufacturing by manipulating substrate temperature and deposition rate. Surface roughness and surface slope are defined as the root-mean-squares of the surface height profile and the surface slope profile, respectively. The dynamics of the evolution of the thin film surface height profile are assumed to be described by an Edwards−Wilkinson-type equation (a second-order stochastic partial differential equation) in two spatial dimensions. Analytical solutions of the expected surface roughness and surface slope are obtained on the basis of the Edwards−Wilkinson equation and are used in the controller design. The model parameters of the Edwards−Wilkinson equation depend on the substrate temperature and deposition rate. This dependence is used in the formulation of the predictive controller to predict the influence of the control action on the surface roughness and slope at the end of the growth process. The model predictive controller involves constraints on the magnitude and rate of change of the control action and optimizes a cost that involves penalty on both surface roughness and mean slope from the set-point values. The controller is applied to the two-dimensional Edwards−Wilkinson equation and is shown to successfully regulate surface roughness and mean slope to set-point values at the end of the deposition that yield desired film reflectance and transmittance.

1. Introduction

Thin film growth of semiconductor materials has attracted significant research attention due to its importance in many applications, such as microelectronic and photovoltaic devices. The microscopic structure and surface morphology of the thin films strongly influence the mechanical, electrical, and photovoltaic properties of the semiconductor devices. For example, the surface roughness, which measures the deviation of the film surface from an ideal one, determines the interfacial properties between two successively deposited layers. Furthermore, recent studies have demonstrated that the light trapping efficiency of thin-film solar cells is determined by the surface roughness and the mean surface slope, the latter of which is the root-mean-square (rms) of the surface slope profile.[1−5]

Toward a rational approach to the manufacturing of thin films with desired surface morphology and film microstructure, significant efforts have been made over the last 10 years in the microscopic modeling and feedback control of thin film growth (see, for example, ref 6 for an overview of key results and references). Modeling approaches can be broadly classified into the following categories: kinetic Monte Carlo (kMC) methods and stochastic differential equation (SDE) models. KMC methods were initially introduced to simulate thin film microscopic processes based on the microscopic rules and the thermodynamic and kinetic parameters obtained from experiments and molecular dynamics simulations.[7−10] Since kMC models are not available in closed form, they cannot be readily used for feedback control design and system-level analysis. On the other hand, SDE models can be derived from the corresponding master equation of the microscopic process[11,12] and/or identified from process data.[6,13] The closed form of the SDE models enables their use as the basis for the design of feedback controllers which can regulate thin film surface roughness (e.g.,[6,13,14]), film porosity,[14,15] and film thickness.[16] Recently, we have initiated an effort toward modeling and control of surface mean slope which strongly influences the light reflectance and transmittance properties of thin films. In this direction, we have studied dynamics and lattice size dependence of surface mean slope[17] and predictive control of both surface roughness and slope using stochastic partial differential equations (PDEs) in one spatial dimension.[18] Recent research work has also focused on the computationally efficient multiobjective optimization and predictive control of microscopic and multiscale systems using in situ adaptive tabulation.[19,20] However, model predictive control of both surface roughness and slope using stochastic PDEs in two spatial dimensions, an important problem from a practical standpoint, to optimize the light trapping efficiency during thin film manufacturing processes has not been studied yet.

This work focuses on the development of a multivariable model predictive controller that simultaneously regulates thin film surface roughness and mean slope to optimize light reflectance and transmittance during thin-film manufacturing by manipulating substrate temperature and deposition rate. The dynamics of the evolution of the thin film surface height profile are assumed to be described by an Edwards−Wilkinson-type equation in two spatial dimensions. Analytical solutions of the expected surface roughness and surface slope are obtained on the basis of the Edwards−Wilkinson equation and are used in the design of a model predictive controller that manipulates substrate temperature and deposition rate. The model predictive controller optimizes a cost that involves penalty on both surface roughness and mean slope from desired set-point values and imposes constraints on the magnitude and rate of change of the control action. The controller is applied to the two-dimensional Edwards−Wilkinson equation and is shown to successfully regulate the surface roughness and mean slope to set-point values

* To whom correspondence should be addressed. Phone: +1 (310) 794-1015. Fax: +1 (310) 206-4107. E-mail: pdc@seas.ucla.edu.
[†] Department of Chemical and Biomolecular Engineering.
[‡] Department of Electrical Engineering.

10.1021/ie100814f
Published on Web 05/12/2010

at the end of the deposition that yield desired film reflectance and transmittance.

2. Preliminaries

2.1. Edwards−Wilkinson Equation for Surface Height Dynamics. The Edwards−Wilkinson (EW) equation, which is a second-order stochastic PDE, has been demonstrated to adequately describe the dynamics of the evolution of the surface height profile in many thin-film growth processes that involve a thermal balance between atom adsorption and surface migration.[17,21−23] In this work, an EW-type equation in two spatial dimensions takes the following form:

$$\frac{\partial h}{\partial t} = c + c_2\left(\frac{\partial^2 h}{\partial x^2} + \frac{\partial^2 h}{\partial y^2}\right) + \xi(x, y, t) \tag{1}$$

where $x \in [0, \pi]$, $y \in [0, \pi]$ are the spatial coordinates, t is the time, $h(x, y, t)$ is the surface height, and $\xi(x, y, t)$ is a Gaussian white noise with a zero mean and the following covariance:

$$\langle \xi(x, y, t)\xi(x', y', t')\rangle = \sigma^2 \delta(x - x')\delta(y - y')\delta(t - t') \tag{2}$$

where $\delta(\cdot)$ denotes the Dirac delta function. c, c_2, and σ^2 are model parameters that have explicit dependence on the macroscopic operating variables, i.e., the substrate temperature, T, and the deposition rate, W. Specifically, c is related to the growth rate of the average surface height and c_2 is related to the effect of surface relaxation/migration. These model parameters can be identified on the basis of kinetic Monte Carlo simulation or experimental data.[13,24] The stochastic PDE of eq 1 is subject to periodic boundary conditions (PBCs) of the form:

$$h(0, y, t) = h(\pi, y, t) \qquad h(x, 0, t) = h(x, \pi, t) \tag{3}$$

$$\frac{\partial h}{\partial x}(0, y, t) = \frac{\partial h}{\partial x}(\pi, y, t) \qquad \frac{\partial h}{\partial y}(x, 0, t) = \frac{\partial h}{\partial y}(x, \pi, t) \tag{4}$$

and the initial condition

$$h(x, y, 0) = h_0(x, y) \tag{5}$$

To analyze the dynamics and obtain a finite-dimensional approximation of the EW equation, we first consider the eigenvalue problem of the linear operator of eq 1 subject to the periodic boundary conditions of eqs 3 and 4:

$$\mathcal{A}\phi_{m,n}(x, y) = c_2\left(\frac{\partial^2}{\partial x^2} + \frac{\partial^2}{\partial y^2}\right)\phi_{m,n}(x, y) = \lambda_{m,n}\phi_{m,n}(x, y) \tag{6}$$

$$\nabla^j \phi_{m,n}(0, y) = \nabla^j \phi_{m,n}(\pi, y), \qquad j = 0, 1 \tag{7}$$

$$\nabla^j \phi_{m,n}(x, 0) = \nabla^j \phi_{m,n}(x, \pi), \qquad j = 0, 1 \tag{8}$$

where $\lambda_{m,n}$ denotes an eigenvalue, $\phi_{m,n}$ denotes an eigenfunction, and ∇^j, $j = 0, 1$, denotes the gradient of a given function. The solution of the eigenvalue problem is as follows:

$$\lambda_{m,n} = 4c_2(m^2 + n^2) \tag{9}$$

$$\phi_{1,m,n} = \frac{2}{\pi}\sin(2mx)\sin(2ny) \tag{10}$$

$$\phi_{2,m,n} = \begin{cases} \dfrac{1}{\pi} & m = 0 \text{ and } n = 0 \\ \dfrac{2}{\pi}\cos(2mx)\cos(2ny) & m \neq 0 \text{ and } n \neq 0 \\ \dfrac{\sqrt{2}}{\pi}\cos(2mx)\cos(2ny) & m = 0, n \neq 0 \text{ or } m \neq 0, n = 0 \end{cases} \tag{11}$$

$$\phi_{3,m,n} = \begin{cases} 0 & m = 0 \\ \dfrac{2}{\pi}\sin(2mx)\cos(2ny) & m \neq 0, n \neq 0 \\ \dfrac{\sqrt{2}}{\pi}\sin(2mx) & m \neq 0, n = 0 \end{cases} \tag{12}$$

$$\phi_{4,m,n} = \begin{cases} 0 & n = 0 \\ \dfrac{2}{\pi}\cos(2mx)\sin(2ny) & n \neq 0, m \neq 0 \\ \dfrac{\sqrt{2}}{\pi}\sin(2ny) & n \neq 0, m = 0 \end{cases} \tag{13}$$

The solution of the EW equation of eq 1 can be expanded in an infinite series in terms of the eigenfunctions of the operator of eq 6 as follows:

$$h(x, y, t) = \sum_{m=0}^{+\infty}\sum_{n=0}^{+\infty} \phi_{1,m,n}z_{1,m,n} + \phi_{2,m,n}z_{2,m,n} + \phi_{3,m,n}z_{3,m,n} + \phi_{4,m,n}z_{4,m,n} \tag{14}$$

where $z_{1,m,n}$, $z_{2,m,n}$, $z_{3,m,n}$, and $z_{4,m,n}$ are time-varying coefficients.

Substituting the above expansion for the solution, $h(x,y,t)$ into eq 1 and taking the inner product with the adjoint eigenfunctions, the following system of infinite stochastic linear ordinary differential equations (ODEs) for the temporal evolution of the time-varying coefficients is obtained:

$$\frac{\mathrm{d}z_{2,0,0}}{\mathrm{d}t} = \pi c + \xi_{2,0,0}(t) \tag{15}$$

$$\frac{\mathrm{d}z_{p,m,n}}{\mathrm{d}t} = \lambda_{m,n}z_{p,m,n} + \xi_{p,m,n}(t), \qquad p = 1, 2, 3, 4, \quad m, n = 0, 1, ..., \infty, \quad m^2 + n^2 \neq 0 \tag{16}$$

where $\xi_{p,m,n} = \int_0^\pi \int_0^\pi \xi(x, y, t)\phi_{p,m,n}\,\mathrm{d}x\,\mathrm{d}y$ is the projection of the noise $\xi(x, y, t)$ on the ODE for $z_{p,m,n}$. The noise term, $\xi_{p,m,n}$, has zero mean and covariance

$$\langle \xi_{p,m,n}(t)\xi_{p,m,n}(t')\rangle = \sigma^2\delta(t - t') \tag{17}$$

The temporal evolution of the variance of mode $z_{p,m,n}$ can be obtained from the solution of the linear ODE of eqs 15 and 16 as follows:

$$\langle ({z_{p,m,n}}^2(t)\rangle = \mathrm{e}^{2\lambda_{m,n}(t-t_0)}\langle ({z_{p,m,n}}^2(t_0)\rangle + \sigma^2\frac{\mathrm{e}^{2\lambda_{m,n}(t-t_0)} - 1}{2\lambda_{m,n}}, \qquad m^2 + n^2 \neq 0 \tag{18}$$

For feedback control purposes (see section 3 below), the modes can be calculated from a surface height measurement as follows:

$$z_{p,m,n}(t) = \int_0^\pi \int_0^\pi h(x, y, t)\phi_{p,m,n}(x, y)\,\mathrm{d}x\,\mathrm{d}y \tag{19}$$

In many circumstances, only discrete height profile measurements are available, thus eq 19 can be approximated by

$$z_{p,m,n}(t) = \frac{\pi^2}{K^2}\sum_{i=0}^{L-1}\sum_{j=0}^{L-1}\hat{h}(i,j,t)\phi_{p,m,n}(i,j) \tag{20}$$

where L is the number of spatial height sampling (measurement) points in $[0, \pi]$ in both x and y coordinates and $\hat{h}(i, j, t) = h(x_i, y_j, t) = h(i\pi/L, j\pi/L, t)$. It is worth pointing out that, when discrete height measurements are available, the highest number of modes that can be accurately calculated is limited by the spatial sampling points, $m, n \le L/2$.

The dependence of c, c_2, and σ^2 on substrate temperature T and deposition rate W can be identified from either experiments or kinetic Monte Carlo simulations of the thin film growth process. The expressions reported in ref 13 that are identified as being from kinetic Monte Carlo simulations are used here:

$$c(T, W) = W\left(1 - \frac{k_w}{W^{a_w}}e^{k_B T/E_w}\right) \tag{21}$$

$$c_2(T, W) = \frac{k_c}{L^2 W^{a_c}}e^{k_B T/E_c} \tag{22}$$

$$\sigma^2(T, W) = \frac{\pi^2}{L^2}[1 + e^{(a_t + k_t W)T - a_v - k_v W}] \tag{23}$$

where k_B is the Boltzmann constant (8.617343×10^{-5} eV/K), $k_w = 3.3829 \times 10^{-12}$, $a_w = 0.6042$, $E_w = 2.7 \times 10^{-3}$ eV, $k_c = 1.0274 \times 10^{-13}$, $a_c = 0.1669$, $E_c = 1.9 \times 10^{-3}$ eV, $a_v = 15.55493$, $k_v = 20.64504$ s, $a_t = 0.02332$ K^{-1}, and $k_t = 0.0261$ s·K^{-1}.

2.2. Film Surface Roughness and rms Slope. Thin-film surface morphology can be characterized by roughness and rms slope. Roughness is defined as the root-mean-square of the surface height profile:

$$\begin{aligned} r(t) &= \sqrt{\frac{1}{\pi^2}\int_0^\pi\int_0^\pi (h(x,y,t) - \bar{h}(t))^2\,dx\,dy} \\ &\approx \sqrt{\frac{1}{L^2}\sum_{i=0}^{L-1}\sum_{j=0}^{L-1}(\hat{h}(i,j,t) - \bar{h})^2} \end{aligned} \tag{24}$$

where $\bar{h}$ denotes the average surface height. Substituting eq 14 into eq 24, the expected value of r^2 can be rewritten in terms of the state covariance as follows:

$$\langle r^2\rangle = \frac{1}{\pi^2}\sum_{m,n=0,m^2+n^2\neq 0}^{L/2}(\langle z_{1,m,n}{}^2\rangle + \langle z_{2,m,n}{}^2\rangle + \langle z_{3,m,n}{}^2\rangle + \langle z_{4,m,n}{}^2\rangle) \tag{25}$$

The rms slope is defined as the root-mean-square of the slope of the surface height:

$$\begin{aligned} m(t) &= \sqrt{\frac{1}{\pi^2}\int_0^\pi\int_0^\pi\left(\frac{\partial h}{\partial x}(x,y,t)\right)^2 dx\,dy} \\ &\approx \sqrt{\frac{1}{\pi^2}\sum_{i=0}^{L-1}\sum_{j=0}^{L-1}\left(\frac{\hat{h}(i+1,j,t) - \hat{h}(i,j,t)}{\Delta x}\right)^2\frac{\pi^2}{L^2}} \end{aligned} \tag{26}$$

The expected rms slope square can also be expressed in terms of the state covariance as follows:

$$\langle m^2\rangle = \sum_{m,n=0,m^2+n^2\neq 0}^{L/2}(K_{1,m,n}\langle z_{1,m,n}{}^2\rangle + K_{2,m,n}\langle z_{2,m,n}{}^2\rangle + K_{3,m,n}\langle z_{3,m,n}{}^2\rangle + K_{4,m,n}\langle z_{4,m,n}{}^2\rangle) \tag{27}$$

where $K_{p,m,n}$ can be computed by

$$K_{p,m,n} = \frac{1}{\pi^2}\sum_{i=0}^{L-1}\sum_{j=0}^{L-1}(\phi_{p,m,n}(i+1,j) - \phi_{p,m,n}(i,j))^2 = \frac{4}{\pi^2}\sin^2\left(\frac{\pi m}{L}\right) \tag{28}$$

3. Multivariable Predictive Controller Design

In this section, a model predictive controller is developed based on the dynamic model of the expected roughness square and rms slope square. Substrate temperature and deposition rate are used as the manipulated variables. The control objective is to minimize the deviation of the expected roughness square and/or rms slope square from desired set-point values. Because the thin film deposition process is a batch process, the interval between current time and the end of the batch run is used as the prediction horizon. During each predictive controller evaluation, the manipulated variable is assumed to stay fixed until the end of the batch. To account for practical considerations, two types of input constrains are imposed. First, both the temperature and the deposition rate have lower and upper limits; second, the rates of change of both inputs are constrained to be less than certain upper limits due to actuator limitations. The resulting MPC formulation is as follows:

$$\min_{T(t),W(t)} J(t) = q_{r^2}(\langle r^2(t_f)\rangle - r_{set}{}^2)^2 + q_{m^2}(\langle m^2(t_f)\rangle - m_{set}{}^2)^2 \tag{29}$$

where

$$\langle r^2(t_f)\rangle = \frac{1}{\pi^2}\sum_{m,n=0,m^2+n^2\neq 0}^{L/2}(\langle z_{1,m,n}{}^2\rangle + \langle z_{2,m,n}{}^2\rangle + \langle z_{3,m,n}{}^2\rangle + \langle z_{4,m,n}{}^2\rangle) \tag{25a}$$

$$\langle m^2(t_f)\rangle = \sum_{m,n=0,m^2+n^2\neq 0}^{L/2}(K_{1,m,n}\langle z_{1,m,n}{}^2(t_f)\rangle + K_{2,m,n}\langle z_{2,m,n}{}^2(t_f)\rangle + K_{3,m,n}\langle z_{3,m,n}{}^2(t_f)\rangle + K_{4,m,n}\langle z_{4,m,n}{}^2(t_f)\rangle) \tag{27a}$$

$$\mathrm{cov}(z_{p,m,n}(t_f)) = e^{-8c_2(m^2+n^2)(t_f-t)}\,\mathrm{cov}(z_{p,m,n}(t)) + \sigma^2\frac{e^{-8c_2(m^2+n^2)(t_f-t)} - 1}{2\lambda_{m,n}}, \qquad m^2 + n^2 \neq 0 \tag{18a}$$

$$c = W\left(1 - \frac{k_w}{W^{a_w}}e^{k_B T/E_w}\right) \tag{21a}$$

$$c_2 = \frac{k_c}{L^2 W^{a_c}}e^{k_B T/E_c} \tag{22a}$$

$$\sigma^2 = \frac{\pi^2}{L^2}[1 + e^{(a_t + k_t W)T - a_v - k_v W}] \tag{23a}$$

subject to

$$c(T, W) \ge c_{min} \tag{30}$$

$$T_{min} \le T \le T_{max}, \qquad W_{min} \le W \le W_{max} \tag{31}$$

$$|T(t) - T(t - dt)| \le \Delta T_{max}, \qquad |W(t) - W(t - dt)| \le \Delta W_{max} \tag{32}$$

where t_f is the final time of the batch run, r_{set}^2 and m_{set}^2 are the respective set-points for the surface roughness square and the mean slope square, q_{r^2} and q_{m^2} are the weighting factors for the deviations of $\langle r^2 \rangle$ and (m^2) from their respective set-points, r_{set}^2 and m_{set}^2, at t_f, dt is the time interval between two successive sampling times and control actions, T_{min} and T_{max} are the lower and upper bounds on the substrate temperature, respectively, ΔT_{max} is the limit on the rate of change of the substrate temperature, W_{min} and W_{max} are the lower and upper bounds on the deposition rate, respectively, and ΔW_{max} is the limit on the rate of change of the deposition rate.

The optimization problem is solved at each sampling time once a new measurement of the surface height profile becomes available. An interior point method optimizer, IPOPT,[25] is used to solve the optimization problem in the MPC formulation.

Remark 1. *Referring to the design and implementation of estimation-based (output feedback) control systems, we note that an output feedback controller, which utilizes a Kalman−Bucy-type filter as the state estimator, was developed and used in the context of covariance control of a stochastic partial differential equation in a previous work of our group.*[26] *Furthermore, estimation-based control of a kinetic Monte Carlo model of a one-dimensional thin-film growth process was also studied in the context of roughness control*[24] *and porosity control.*[27] *In the present work, we focus on the model predictive control of surface roughness and slope of a process described by the Edwards−Wilkinson equation in two spatial dimensions. The application of the proposed controller to a kinetic Monte Carlo simulation model of a two-dimensional thin-film growth process, as well as the design of an estimation-based control scheme, will be addressed in a future work.*

4. Simulation Results

In this section, the model predictive controller of eq 29 is applied to the two-dimensional EW equation plant model of eq 1. The variation of substrate temperature is from 600−750 K, and the variation of the deposition rate is from 0.1 to 1 layer/s. The initial temperature is 610 K, and the initial deposition rate is 1 layer/s. The maximum rates of change is $T_{max} = 5$ K/s for temperature and $\Delta W_{max} = 0.05$ layer/s for deposition rate. The sampling time is 5 s. Each closed-loop simulation lasts for 100 s. Expected values are calculated from 100 independent runs.

4.1. Control of Film Surface Roughness. First, the problem of regulating film surface roughness is considered. In this scenario, the cost function only contains penalty on the deviation of the expected surface roughness square from the set-point. The weighting factors are $q_{r^2} = 1$ and $q_{m^2} = 0$. The set-point is $r_{set}^2 = 15$.

Figure 1 shows the profile of $\langle r^2 \rangle$ under the model predictive controller of eq 29. It can be seen that the controller drives the expected film roughness at the end of the simulation close to the desired value. Figure 2 shows the expected profiles of T and W for the closed-loop simulation. The overall variations of both temperature and deposition rate are small because the initial values of these variables are close to the ones needed to accomplish the desired set-points for surface roughness and slope. As a result, the constraints on the rate of change of the manipulated variables are not reached in this case since the rates of change of the variables requested by the controller are much smaller than the imposed constraints. Figure 3 compares the histogram of r^2 from open-loop and closed-loop simulations. The model predictive control algorithm reduces the variance of r^2 by 47%, from 0.3179 to 0.1681.

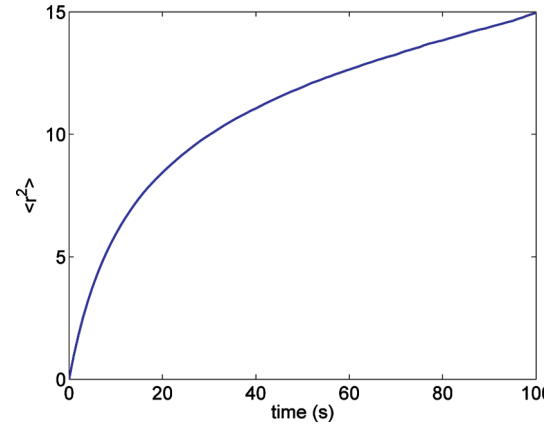

Figure 1. Profile of expected film surface roughness square from 100 closed-loop simulations. $q_{r^2} = 1$, $q_{m^2} = 0$, and $r_{set}^2 = 15$.

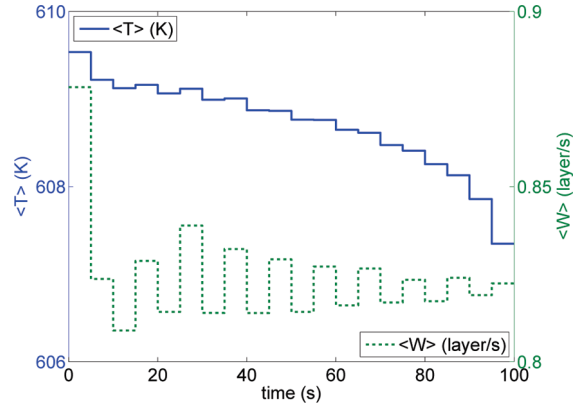

Figure 2. Profiles of manipulated variables. $q_{r^2} = 1$, $q_{m^2} = 0$, and $r_{set}^2 = 15$.

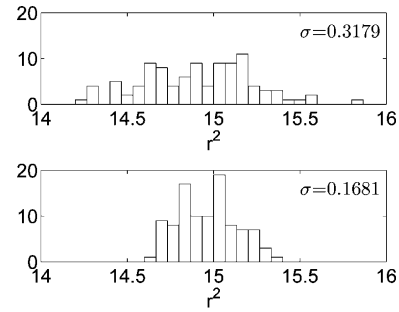

Figure 3. Comparison of histograms of r^2 at the end of the simulation between open-loop (top plot) and closed-loop (bottom plot) simulations. $q_{r^2} = 1$, $q_{m^2} = 0$, and $r_{set}^2 = 15$.

4.2. Control of Film Surface rms Slope. Next, we consider the regulation of thin film surface rms slope. The cost function includes only penalty on the deviation of the expected value of rms slope square from the set point by choosing weighting factors $q_{r^2} = 0$ and $q_{m^2} = 1$. The set point is $m_{set}^2 = 0.2$.

Figure 4 shows the profile of expected rms slope square from 100 repeats of closed-loop simulations. The rms slope reaches its set point at $t = 100$ s. The constraint on the rate of change of the temperature takes effect in the slope-only control problem and limits the increase of the substrate temperature at the initial stage of the deposition. A peak appears in the slope profile in

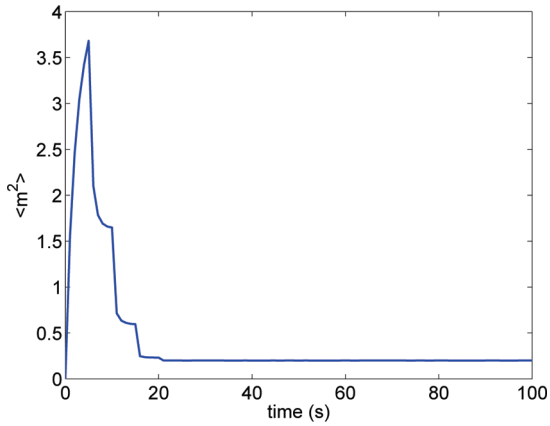

Figure 4. Profile of expected film surface rms slope square from 100 closed-loop simulations. $q_{r^2} = 0$, $q_{m^2} = 1$, and $m_{set}^2 = 0.2$.

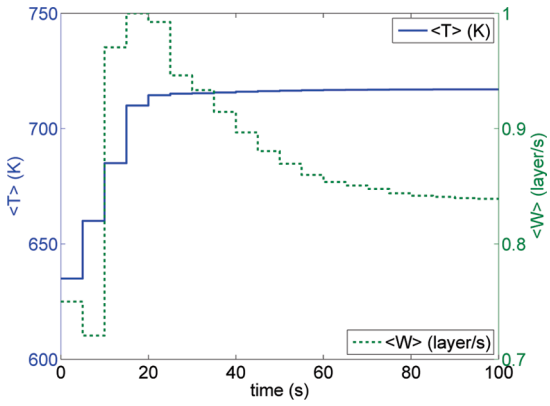

Figure 5. Profiles of manipulated variables. $q_{r^2} = 0$, $q_{m^2} = 1$, and $m_{set}^2 = 0.2$.

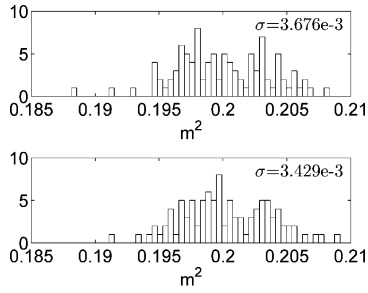

Figure 6. Comparison of histograms of m^2 at the end of the simulation between open-loop (top plot) and closed-loop (bottom plot) simulations. $q_{r^2} = 0$, $q_{m^2} = 1$, and $m_{set}^2 = 0.2$.

the first 20 s because the temperature can not increase fast enough from its initial value due to the rate of change constraint. Figure 5 shows the profile of expected temperature and deposition rate. Because the low set-point value of the mean slope square requires a relatively high substrate temperature, the controller increases the temperature at the maximum rate during the first four steps and then keeps the temperature around 716 K. The comparison of histograms of m^2 at the end of the simulation between closed-loop and open-loop is presented in Figure 6. The MPC reduces the variance but by a smaller amount compared to the case of roughness-only control.

4.3. Simultaneous Control of Roughness and rms Slope. Finally, simultaneous regulation of roughness and rms slope is carried out. The set-points of the surface roughness square and of the mean slope square are $r_{set}^2 = 15$ and $m_{set}^2 =$

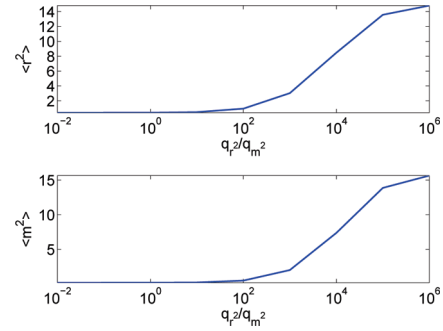

Figure 7. $\langle r^2 \rangle$ and $\langle m^2 \rangle$ at the end of closed-loop simulations ($t = 100$ s) for different penalty weighting factors: $q_{m^2} = 1$ and $0.01 \le q_{r^2} \le 10^6$.

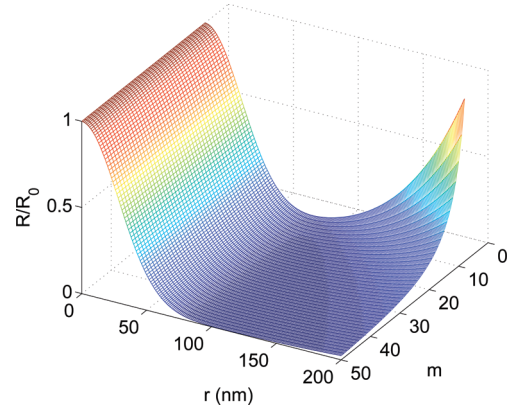

Figure 8. Reflectance as a function of r and m of the thin-film surface.

0.2. The weighting factor of mean slope square is kept at 1, while the weighting factor of roughness square increases from 0.01 to 10^6.

Figure 7 shows the change of $\langle r^2 \rangle$ and $\langle m^2 \rangle$ as a function of q_{r^2}/q_{m^2}. It can be seen that as the weighting on roughness square increases, the expected roughness square approaches more closely its set-point value at the cost of larger deviation of rms slope square from its set-point value.

4.4. Application to Light Trapping Efficiency. For thin-film solar cells, the energy conversion efficiency is directly related to the light trapping/scattering properties of the thin film interfaces and surfaces, which can be characterized by the roughness, r, and the rms slope, m. Specifically, Rayleigh scattering occurs when the incident light goes through a rough interface where it is divided into four components: specular reflection, specular transmission, diffused reflection, and diffused transmission.[28,29] If a rough thin-film surface is illuminated with a beam of monochromatic light at normal incidence, the total reflectance, R, can be approximately calculated as follows:[30]

$$R = R_0 \exp\left[-\frac{4\pi r^2}{\lambda^2}\right] + R_0 \int_0^{\pi/2} 2\pi^4 \left(\frac{a}{\lambda}\right)^2 \left(\frac{r}{\lambda}\right)^2 (\cos\theta + 1)^4 \sin\theta \times \exp\left[-\frac{(\pi a \sin\theta)^2}{\lambda^2}\right] d\theta \qquad (33)$$

where R_0 is the reflectance of a perfectly smooth surface of the same material, r is the roughness, θ is the incident angle, λ is the light wavelength, and a is the autocovariance length. It can be proved that $a = (2)^{1/2} r/m$, where m is the rms slope of the profile of the surface.[31] The numerical integration result of eq 33 is shown in Figure 8. From this plot, it can be inferred that both r and m strongly influence the intensity of light reflection (and, therefore, light transmission) by the surface/interface. Thus, it is important to regulate r and m of the surfaces/interfaces of

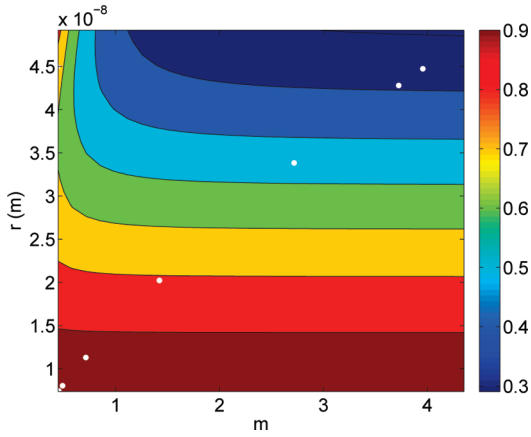

Figure 9. Light reflectance of thin films deposited under closed-loop operations with different weighting factor ratio.

the thin-film solar cells to appropriate values that optimize light reflectance and transmittance during thin film manufacturing.

In the simultaneous control of roughness and slope in section 4.3, the expected surface roughness square and mean slope square can be regulated to different levels with the same set-points by choosing different weighting schemes, i.e., different ratios between the weighting factors, q_{r^2}/q_{m^2}. The corresponding light reflectance for different weighting factor ratios can be computed according to eq 33. In Figure 9, the roughness and rms slope obtained from closed-loop simulations with different q_{r^2}/q_{m^2} are mapped to a contour of reflectance. Note that the roughness is scaled by a factor of 1.16×10^{-8} m to represent the length scales of atomic particles in thin film growth processes. We can see that by changing the ratio, q_{r^2}/q_{m^2}, we can produce films whose surface leads to different reflectance values.

Remark 2. *Certain set-points for both surface roughness and surface slope are desired to be attained during the manufacturing (thin-film growth) process to optimize the light trapping efficiency of thin-film solar cells. These requirements may be attained through penalty of the deviation of surface roughness and slope in the cost functional (as done in this work) or through imposition of explicit "soft" or "hard" constraints on these variables in the model predictive control problem. The latter approach may be more suitable in applications where there is a need to achieve a roughness (slope) level less than a maximum acceptable roughness (slope) level.*

5. Conclusion

In this work, a multivariable model predictive controller was developed to simultaneously regulate thin-film surface roughness and mean slope to optimize film light reflectance and transmittance during thin-film manufacturing. The dynamics of the evolution of the thin-film surface height profile were assumed to be described by an EW-type equation in two spatial dimensions. Analytical solutions of the expected surface roughness and surface slope were obtained on the basis of the EW equation and were used in the design of model predictive controller that manipulates the substrate temperature and deposition rate. The model predictive controller involves constraints on the magnitude and rate of change of the control action and optimizes a cost that involves penalty on both surface roughness and mean slope from the set-point values. The controller was applied to the two-dimensional Edwards−Wilkinson equation and was demonstrated to successfully regulate surface roughness and mean slope to set-point values at the end of the batch operation that yield desired film reflectance and transmittance.

Literature Cited

(1) Zeman, M.; Vanswaaij, R. Optical modeling of a-Si: H solar cells with rough interfaces: Effect of back contact and interface roughness. *J. Appl. Phys.* **2000**, *88*, 6436–6443.

(2) Poruba, A.; Fejfar, A. Optical absorption and light scattering in microcrystalline silicon thin films and solar cells. *J. Appl. Phys.* **2000**, *88*, 148–160.

(3) Müller, J.; Rech, B.; Springer, J.; Vanecek, M. TCO and light trapping in silicon thin film solar cells. *Solar Energy* **2004**, *77*, 917–930.

(4) Springer, J.; Poruba, A. Improved three-dimensional optical model for thin-film silicon solar cells. *J. Appl. Phys.* **2004**, *96*, 5329–5337.

(5) Rowlands, S. F.; Livingstone, J.; Lund, C. P. Optical modelling of thin film solar cells with textured interfaces using the effective medium approximation. *Solar Energy* **2004**, *76*, 301–307.

(6) Christofides, P. D.; Armaou, A. Control and optimization of multiscale process systems. *Comp. Chem. Eng.* **2006**, *30*, 1670–1686.

(7) Levine, S. W.; Engstrom, J. R.; Clancy, P. A kinetic Monte Carlo study of the growth of Si on Si(100) at varying angles of incident deposition. *Surf. Sci.* **1998**, *401*, 112–123.

(8) Zhang, P.; Zheng, X.; Wu, S.; Liu, J.; He, D. Kinetic Monte Carlo simulation of Cu thin film growth. *Vacuum* **2004**, *72*, 405–410.

(9) Levine, S. W.; Clancy, P. A simple model for the growth of polycrystalline Si using the kinetic Monte Carlo simulation. *Modell. Simul. Mater. Sci. Eng.* **2000**, *8*, 751–762.

(10) Christofides, P. D.; Armaou, A.; Lou, Y.; Varshney, A. *Control and Optimization of Multiscale Process Systems*; Birkhäuser: Boston, 2008.

(11) Haselwandter, C. A.; Vvedensky, D. D. Renormalization of stochastic lattice models: Basic formulation. *Phys. Rev. E* **2007**, *76*, 041115.

(12) Haselwandter, C. A.; Vvedensky, D. D. Renormalization of stochastic lattice models: Epitaxial surfaces. *Phys. Rev. E* **2008**, *77*, 061129.

(13) Ni, D.; Christofides, P. D. Multivariable Predictive Control of Thin Film Deposition Using a Stochastic PDE Model. *Ind. Eng. Chem. Res.* **2005**, *44*, 2416–2427.

(14) Hu, G.; Orkoulas, G.; Christofides, P. D. Stochastic modeling and simultaneous regulation of surface roughness and porosity in thin film deposition. *Ind. Eng. Chem. Res.* **2009**, *48*, 6690–6700.

(15) Hu, G.; Orkoulas, G.; Christofides, P. D. Modeling and control of film porosity in thin film deposition. *Chem. Eng. Sci.* **2009**, *64*, 3668–3682.

(16) Hu, G.; Orkoulas, G.; Christofides, P. D. Regulation of film thickness, surface roughness and porosity in thin film growth using deposition rate. *Chem. Eng. Sci.* **2009**, *48*, 3903–3913.

(17) Huang, J.; Hu, G.; Orkoulas, G.; Christofides, P. D. Lattice-size dependence and dynamics of surface mean slope in a thin film deposition process. *Proceedings of 9th IFAC Symposium on Dynamics and Control of Process Systems*, Leuven, Belgium, 2010, in press.

(18) Zhang, X.; Hu, G.; Orkoulas, G.; Christofides, P. D. Predictive control of surface mean slope and roughness in a thin film deposition process. *Chem. Eng. Sci.*, accepted.

(19) Varshney, A.; Armaou, A. Multiscale optimization using hybrid PDE/kMC process systems with application to thin film growth. *Chem. Eng. Sci.* **2005**, *60*, 6780–6794.

(20) Varshney, A.; Armaou, A. Reduced order modeling and dynamic optimization of multiscale PDE/kMC process systems. *Comput. Chem. Eng.* **2008**, *32*, 2136–2143.

(21) Edwards, S. F.; Wilkinson, D. R. The surface statistics of a granular aggregate. *Proc. R. Soc. London Ser. A−Math. Phys. Eng. Sci.* **1982**, *381*, 17–31.

(22) Family, F. Scaling of rough surfaces: effects of surface diffusion. *J. Phys. A: Math. Gen.* **1986**, *19*, L441–L446.

(23) Hu, G.; Huang, J.; Orkoulas, G.; Christofides, P. D. Investigation of film surface roughness and porosity dependence on lattice size in a porous thin film deposition process. *Phys. Rev. E* **2009**, *80*, 041122.

(24) Hu, G.; Lou, Y.; Christofides, P. D. Model parameter estimation and feedback control of surface roughness in a sputtering process. *Chem. Eng. Sci.* **2008**, *63*, 1810–1816.

(25) Wächter, A.; Biegler, L. On the implementation of an interior-point filter line-search algorithm for large-scale nonlinear programming. *Math. Progr.* **2006**, *106*, 25–57.

(26) Hu, G.; Lou, Y.; Christofides, P. D. Dynamic output feedback covariance control of stochastic dissipative partial differential equations. *Chem. Eng. Sci.* **2008**, *63*, 4531–4542.

(27) Zhang, X.; Hu, G.; Orkoulas, G.; Christofides, P. D. Controller and estimator design for regulation of film thickness, surface roughness

and porosity in a multiscale thin film growth process. *Ind. Eng. Chem. Res.* **2010**, in press. doi: 10.1021/ie901396g.

(28) Tao, G.; Zeman, M. Optical modeling of a-Si:H based solar cells on textured substrates *1994 IEEE First World Conference on Photovoltaic Energy Conversion. Conference Record of the Twenty Fourth IEEE Photovoltaic Specialists Conference-1994 (Cat. No. 94CH3365-4)*; **1994**; Vol. 1, p 666.

(29) Leblanc, F.; Perrin, J. Numerical modeling of the optical properties of hydrogenated amorphous-silicon-based p-i-n solar cells deposited on rough transparent conducting oxide substrates. *J. Appl. Phys.* **1994**, *75*, 1074–1087.

(30) Davies, H. The reflection of electromagnetic waves from a rough surface. *Proc. Inst. Electr. Eng.* **1954**, *101*, 209–214.

(31) Bennett, H. E.; Porteus, J. O. Relation between surface roughness and specular reflectance at normal incidence. *J. Opt. Soc. Am.* **1961**, *51*, 123–129.

Received for review April 4, 2010
Revised manuscript received April 27, 2010
Accepted April 27, 2010

IE100814F